MSEC2021-XXXX

ADHESIVE DEPOSITION PROCESS CHARACTERIZATION FOR MICROSTRUCTURE ASSEMBLY

Andriy Sherehiy Louisville Automation and Robotics Research Institute, University of Louisville Louisville, KY

Andres Montenegro Department of Mechanical Engineering, University of Louisville, Louisville, KY

Danming Wei Louisville Automation and Robotics Research Institute, University of Louisville, Louisville, KY

Dan O. Popa Louisville Automation and Robotics Research Institute, University of Louisville, Louisville, KY

ABSTRACT

Recent advancements in additive manufacturing such as Direct Write Ink Jet printing, introduced novel tools that. allow controlled and precise deposition of fluid in nano-Liter volumes, enabling fabrication of multiscale structures with submillimeter dimensions. Applications include fabrication of flexible electronics, sensors, and assembly of Micro-Electro-Mechanical Systems (MEMS). Critical challenges remain in the control of fluid deposition parameters during Inkjet printing to meet specific dimensional footprints at the microscale necessary for the assembly process of microscale structures. In this paper we characterize an adhesive deposition printing process with a piezo-electric dispenser of nano-liter volumes. Applications include the controlled delivery of high viscosity Ultraviolet (UV) and thermal curable adhesives for the assembly of the MEMS based structures. We applied the Taguchi Design of Experiment (DOE) method to determine optimal set of process parameters required to minimize the size of adhesive printed features on a silicon substrate with good reliability and repeatability of the deposition process. Experimental results presented in this paper demonstrate repeatable deposition of UV adhesive features with 150 µm diameter on the silicon substrate. Based on the observed wettability effect of adhesive printed onto the different substrates we propose solution for further reduction of the deposit-substrate contact area for microassembly optimization and flexibility.

Keywords: additive manufacturing, direct write Ink Jet printing, design of experiment (DOE), microassembly, MEMS

1. INTRODUCTION

A common challenge associated with microsystems assembly is the need for high precision positioning over a large area, relative to individual component size. This challenge is usually addressed by developing coherent assembly tools and

processes at multiple scales using parallel assembly and modular design. These designs enable high-throughput, fault-tolerant assembly at moderate cost, and frequently microsystem assembly cells for small-batch production [1, 2]. Following this approach of flexible manufacturing of 3D Micro-Electro-Mechanical-System (MEMS), modular assembly process have been proposed based on compliant sockets and connectors that allow micromechanical component to self-align [3]. Although the compliant snap fasteners are used to temporarily hold the assemblies in place, it is also necessary to increase the bonding strength of assemblies to survive vibration, shock or microactuator motion [4]. Joining and locking of Silicon microscopic parts can be realized with the help of deposited solder alloy layers which are reflowed after assembly [5]. However, this process is costly, and involves exposing components to high temperatures.. Ultraviolet (UV) adhesive is an alternative to soldering with the added benefit of reduced process time, cost and exposure temperatures. Due to its low curing temperature application of UV glue allows to avoid potential damage of parts being joined [6]. An additional advantage is that bonding occurs over the entire surface area of the joint, rather than in discrete spots or along seams, thereby distributing stresses over the entire area where joint design is often simplified [7].

Currently micro-fasteners are used in the assembly of microrobots developed by our group, in particular the Solid Articulated Four Axis Microrobot (sAFAM). sAFAM is a novel 3D-assembled microrobot with four degrees of freedom suitable for manipulation of nano/microscale scale objects [8,9] (Figure 1). The microrobots components are fabricated on a Silicon on Insulator (SOI) wafer with 100 μ m thick device layer, then released and assembled using a custom passive microgripper mounted with the help of on a custom robotic microassembly station [8-11]. Figure 2 shows assembled silicon microparts of

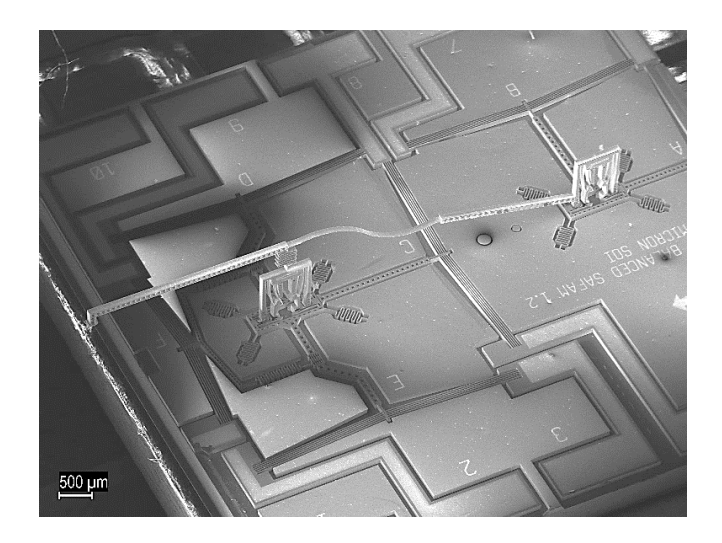


FIGURE 1: SEM IMAGE OF ILLUSTRATION OF A FULLY ASSEMBLED SAFAM MICROROBOT.

sAFAM component where snap-fastening connectors are bonded with the help of UV adhesive.

A critical requirement of completed MEMS assemblies is the alignment of snap-fastened connectors due to induced stresses during UV adhesive curing process [12,13]. To mitigate this challenge, the deposition volume (droplet size) needs to be reduced as much as possible. Flexible and cost-effective solutions for adhesive dispensing can be direct write InkJet printing, a process which so far was successfully applied in fabrication and integration of the microscale structures [14,15]. In this paper we propose to use Inkjet printing as the method for controlled dispensing of small volumes of UV adhesive which will also lead to the overall automation of the microrobot manufacturing process. Dispensing of adhesive was realized using a Nordson EFD® Pico Pulse system, which is controlled by a number of process variables. We applied the Taguchi Design of Experiment (DOE) method in order to identify process parameters needed for reducing the size of adhesive droplets (deposits) [16 - 18] and conduct characterization of the printed features with the help of optical microscopy and scanning electron microscopy (SEM).

The paper is organized in the following way: in Section 2, we describe our experimental set up and experimental methods: deposition process and characterization of the samples. Section 3 presents experimental results and details application of Taguchi DOE method. In Section 4 we discuss our results and optimization of the deposition process in context Taguchi method and micro assembly. Finally, in Section 5, we conclude the paper and discuss future work.

2. MATERIALS AND METHODS

2.1 Experimental setup

A pneumatic Pico Pulse® InkJet instrument manufactured by Nordson EFD, Westlake, OH, was used to design and conduct adhesive deposition experiments. The experimental setup is

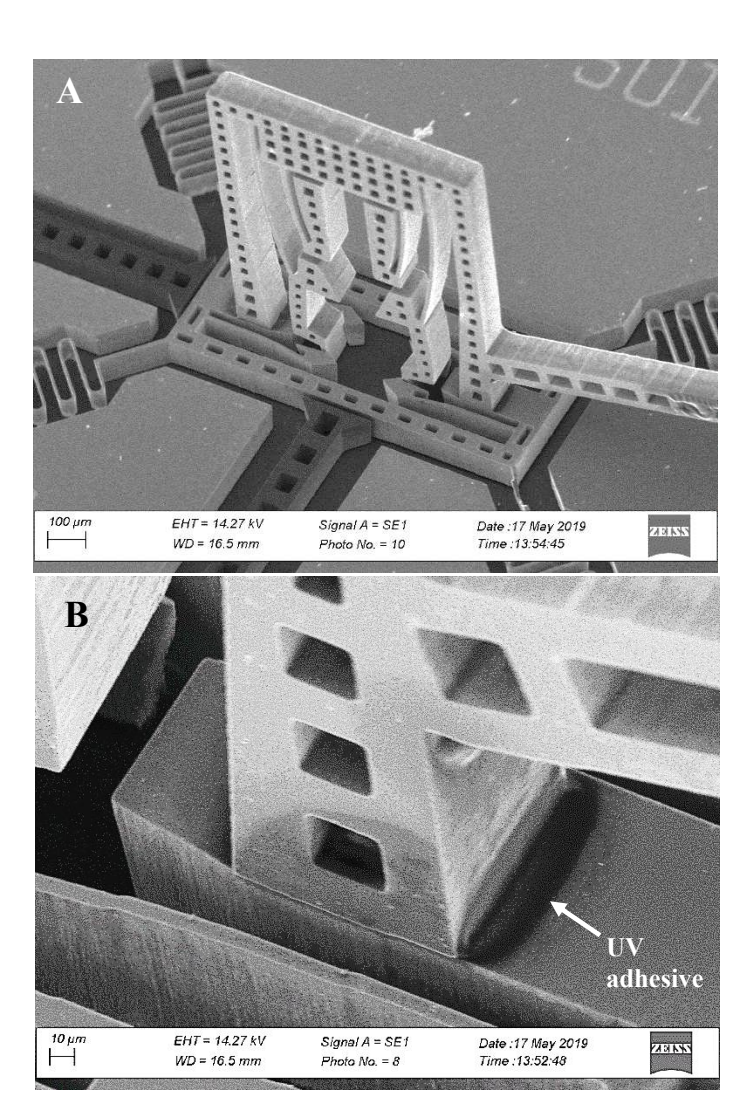
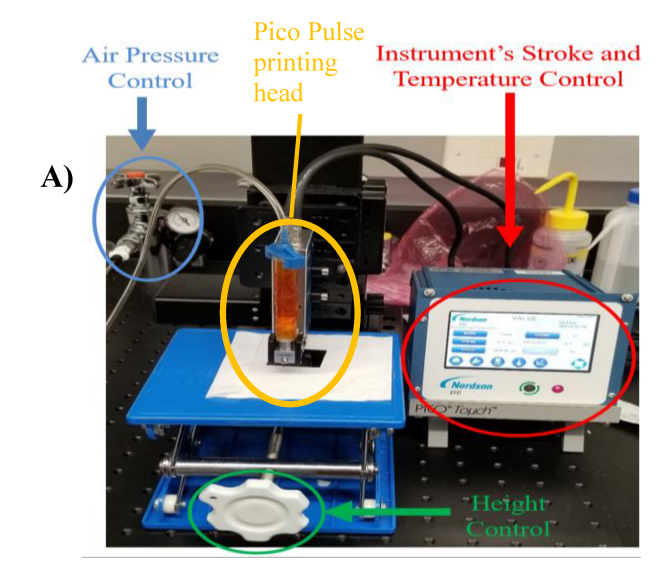


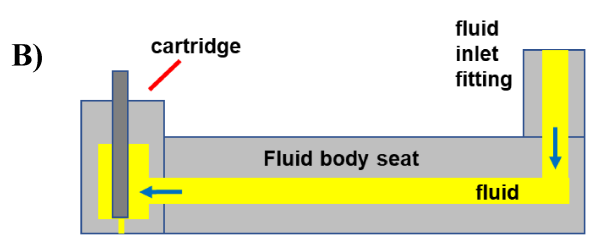
FIGURE 2: SEM IMAGES OF SAFAM'S COMPONENT WHERE TWO MICROSCOPIC PARTS ARE FASTENED USING COMPLIANT INSERTION. A) VIEW OF THE WHOLE ASSEMBLY, B) DETAIL SHOWING POINT OF CONTACT BETWEEN TWO SEPARATE SI PARTS WITH VISIBLE UV ADHESIVE RESIDUE.

shown in Figure 3, depicting the following major system components:

- Pico Pulse print head with piezoelectric actuator, fluid syringe, and valve assembly with 50 µm nozzle.
- Nordson EFD Pico Pulse controller.
- Sample vertical displacement stage to control sample height.
- Air pressure gauge.

The Pico Pulse printing head consists of a piezoelectric mechanism (actuator), and a valve assembly. The valve assembly's main components include a fluid body seat, cartridge, and fluid inlet fitting (Figure 3C).





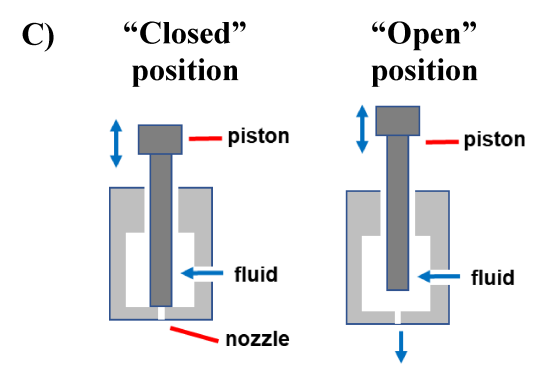


FIGURE 3: A) PICO PULSE EXPERIMENTAL SET UP, B) SCHEMATIC VIEW, CROSS SECTION OF VALVE ASSEMBLY, C) CARTRIDGE AND POSITION OF ITS PISTON IN CLOSED AND OPEN MODE.

Based on information provided by manufacturer, the fluid deposition with the help of print head is realized in the following way (Figure 3C):

- Initially, the piezoelectric actuator is engaged, which keeps a piston tip in the "Close" position and prevents fluid from entering the nozzle opening.
- When the piezoelectric actuator is disengaged, it retracts a piston tip by a specific distance (Δl) from nozzle opening, and it is in an "Open" position. The value of Δl depends on the voltage applied to actuator (Figure 3 C),

- The retracted piston enables a portion of the dispensed fluid to enter the fluid body seat and nozzle opening. Next, the actuator is engaged again,
- which results in piston's tip forcing fluid into the nozzle opening and sealing it off from the fluid reservoir.

The timeline of the controlled deposition cycle is described in the Figure 4. Schematic plot shows the piezoelectric actuator voltage drops during the "open" operation releasing the piston. During "close" section of the deposition cycle actuator is engaged again by increasing the voltage which results in sealing off the nozzle.

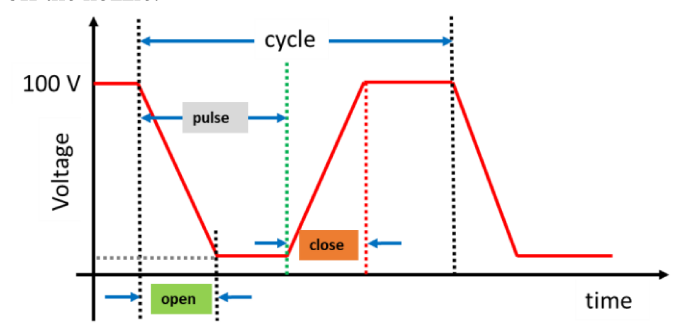


FIGURE 4: DESCRIPTION OF THE PICO PULSE FLUID DISPENSE CYCLE ON A TIME SCALE.

The fluid dispensing process is controlled by the following process parameters:

- Air Pressure, p_a (20psi 100psi): Pressurized air is used to push the force through the chambers of the valve assembly.
- Pulse Time (0.27ms 0.52ms): Pulse time determines how long the valve will be open allowing release of the fluid (Figure 4).
- Open time (0.25ms 0.50ms): The time taken to drive the piston up to the specified stroke (Figure 3C and 4).
- Close time (0.20ms 0.40ms): Is the quantity that determines how long it will take the piston to travel from the specified stroke position to close off the orifice while pushing the collected fluid through the nozzle (Figure 3C and 4).
- Voltage, V (Change in voltage ≤ 90V): Difference between voltage values in "open" and "closed" modes (Figure 4). In closed mode usually 100 110 V is applied to engage piezoelectric mechanism securing the piston to the nozzle orifice. Open mode (position) will correspond to a lower voltage (≤ 90 V) due to relaxation of the piezoelectric actuator releasing the piston from nozzle opening allowing the flow of the fluid.
- Stroke (50% 90% of 100V): This parameter refers to the percentage change between open and closed voltage ΔV determining how far the piston is retracted from the nozzle opening. It can also be thought of as travel distance Δl of the piston 90% will correspond to a larger distance Δl between piston's tip and nozzle's opening allowing the release of larger volume of the fluid. For example: Stroke

- = 90% would correspond to the value of voltage, 10 V (applied to piezoelectric actuator). At stroke of 90% (10V) piston would be retracted to the maximum position of Δl the farthest from the nozzle opening.
- Deposition Height (1 mm 5 mm): The distance from the printer head's nozzle to the substrate.
- Temperature (30 °C 75 °C): The temperature of the heater body and fluid.

The instrument's stroke, pressure p_A , temperature T_f , and deposition height h were chosen as the candidate experimental parameters with significant impact on adhesive droplet's diameter d_d reduction.

2.2 Taguchi Design of Experiments

A trial-error study to evaluate process factors is impractical and time consuming in the case of processes with a large number of experimental parameters (>3). Taguchi approach is a robust statistical method for designing a process that has a minimum sensitivity to variations of uncontrollable experimental factors (noise), and concentrates on main effect estimation of control parameters (signal) using acceptable signal-to-noise ratios S/N. In the Taguchi method, impact of each experimental factor is studied by variating "response" choosing an adequate signal-tonoise (S/N) ratio. The S/N, which is defined as the ratio of signal power (the mean) to noise power corrupting the signal (the standard deviation), is an output response of a selected system and a measure for the robustness of the system. Generally, three S/N formulas are usually used: smaller-the-better response, larger-the-better response, and nominal-the-best response [17, 18]. Since our ultimate goal is optimization of the InkJet printing process in order to reduce size of the droplet, in this study we use smaller-the-better S/N ratio described by the following equation [16,17]:

$$S/N = -10Log\left(\frac{1}{N}\sum_{i=1}^{N}y_i^2\right)$$
 (1) where, y_i is and i^{th} observation and N is a total number of

where, y_i is and i^{th} observation and N is a total number of observations in the experiment. In our case y_i corresponds to measured diameter of the deposited adhesive feature in the substrates plane – usually of approximately circular shape (Figure 5).

For our application, an initial Taguchi Design of Experiment (DOE) with four parameters and three levels sets for deposition of adhesives was used to understand adhesive parameter tendencies toward deposition diameter reduction. The Taguchi DOE method helped to identify appropriate levels of each control parameter and to determine which parameters have statistically significant effects on the reduction of adhesive droplet diameter. Taguchi DOE statistical analysis was performed with the help of MiniTab® software.

2.3 Experimental procedures

Adhesive droplets were deposited on two different types of substrate: glass and silicon (microscope glass slides and 500 μm Si wafers). It is crucial to degrease and clean the surface from any possible impurities or particles that might affect adhesive bonding and droplet diameter. Cleaning the silicon wafers for

deposition substrate was achieved using a sonicator for a five-minute Acetone bath, followed by a five-minute Isopropyl Alcohol (IPA) bath, and finally a five-minute rinse with deionized water. Surface air gun drying occurred after each bath. The clean silicon wafers were stored in clean cases until ready for use.

Bondic® UV/thermal adhesive, from Parker-Lord, Cary, NC, with viscosity of 5000 cPs, comes in an air sealed container; however, the presence of trapped air bubbles might taint the fluid motion through the PICO Pulse valve assembly. A common practice is to remove as much air as possible by using a vacuum chamber. After the air was removed the whole adhesive syringe body was wrapped with Kapton tape with the intention of insulating and protecting from light. Curing is a crucial step for increasing adhesive bonding strength. The Bondic® UV/thermal adhesive manufacturer recommended using an ultraviolet flashlight capable of producing a wavelength of 350 nm to 380 nm for a suggested 90 second UV curing time.

Our deposition experiments were carried out using cleaned microscope glass slides. When optimal sets of parameters was determined, we used Silicon samples of a size 2 cm x 2cm for the final set of trials. Glass slides and silicon wafers that contain adhesive droplets with certain parameter combinations were classified by trial numbers and stored on glass slide containers for deposition characterization.

Metrology data (adhesive droplet diameters) was collected using an optical microscope and scanning electron microscope. An Olympus BX51 microscope was used for immediate imaging and microscopic measurement of adhesive droplet diameters. SEM Zeiss Supra 35 was used for the profile characterization of the droplets. For SEM characterization we have coated UV adhesive samples with ~20 nm conducting layer of the Au/Pd to optimize imaging process. After analyzing multiple trial numbers and identifying the adhesive behavior, a new set of DOEs was tested with new parameters towards droplet diameter reduction. From the last set of DOEs, the data collected enable determination of parameters that induced droplet size. A final set of trials was performed with the best combination of parameters for repeatability and reliability purposes on a cleaned (degreased) silicon substrates.

3. RESULTS

Following the collection the characterization data - droplet diameters d_d for each combination of parameters, we have performed Taguchi DOE analysis with four parameters and three levels. The initial Taguchi DOE testing parameters and control levels were:

- Stroke: 80%100V, 85%100V, and 90%100V.
- Air Pressure: 40 psi, 60 psi, and 80 psi.
- Temperature: 35°C, 45°C, and 55°C.
- Deposition Height: 1 mm, 3 mm, and 5 mm.

The collected results of the d_d and values of respective parameters for the initial Taguchi DOE is shown in Table 1.

Table 1: Initial Taguchi DOE data for UV adhesive droplets on the glass substrate.

Testing Line	Stroke	Air Pressure, pa [psi]	Fluid Temperature, T _f [°C]	Deposition Height, h [mm]	Diameter, d _{d1} (μm)	Diameter, d _{d2} (μm)	Diameter, d _{d3} (μm)
1	80%	40	35	1	-	-	-
2	80%	60	45	3	383.0	379.0	381.0
3	80%	80	55	5	392.5	396.5	409.9
4	85%	40	45	5	383.1	379.0	387.1
5	85%	60	55	1	409.9	414.0	423.4
6	85%	80	35	3	385.2	389.8	380.4
7	90%	40	55	3	396.5	399.2	409.9
8	90%	60	35	5	369.6	349.5	352.2
9	90%	80	45	1	319.9	325.3	332.5

In Figure 5 we present microscope images of the deposited UV adhesive droplets on the glass substrate. Results of statistical analysis and ranking for significant effects on the value of adhesive droplet diameter are collected in Table 2. The largest diameter of the adhesive droplet appears to be deposited at the temperature of 55°C, meanwhile the smallest diameter corresponds to the stroke of 90%. The most significant change of the diameter is observed for the temperature parameter $T_{\rm f}$ (Figure 6, Table 2) indicating that temperature of the fluid has a strongest impact on droplet's size during deposition process.

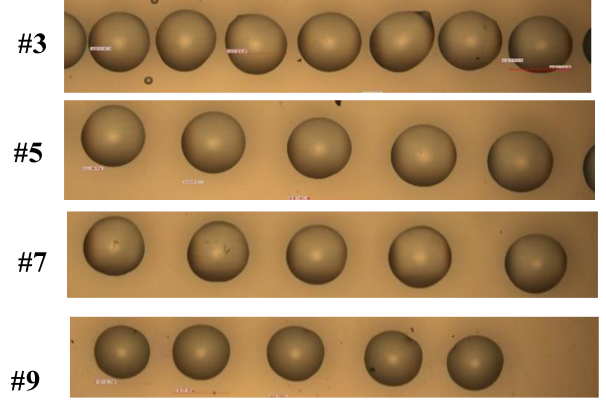


FIGURE 5: MICROSCOPE IMAGES OF THE DEPOSITED UV GLUE DROPLETS ON GLASS SUBSTRATE. NUMBER OF THE IMAGE CORRESPONDS TO THE SPECIFIC SET OF PARAMETERS IN THE TABLE 1. SCALE BAR CORRESPONDS TO 400 MICRON.

Table 2: Response table for means from initial Taguchi DOE.

Level	Stroke	Air Pressure, pa [psi]	Temp., T _f	Deposition height, h [mm]
1	390	392	371	371
2	395	385	363	389
3	362	370	406	380
Δd_{mean}	33	22	43	18
Rank	2	4	1	3

In Table 2, $\Delta d_{mean} = (\Delta d_{mean, Max} - \Delta d_{mean, Min})$ represents mean change (variance) and indicates level of each parameter's impact on droplet sizes. Bigger variances in diameters for a given parameter would result in a bigger value for Δd_{mean} , Thus, the parameter with the biggest mean variance value is ranked as the one with the most impact on the droplet diameters, and the parameter with the smallest Δd_{mean} value - has the least impact. From Table 2 is shown that Temperature and Instrument's Stroke have the larger values of Δd_{mean} (rank 2 and 1) hence strong correlation with droplet size change, meanwhile Deposition Height and Air Pressure have the least impact on droplet size.

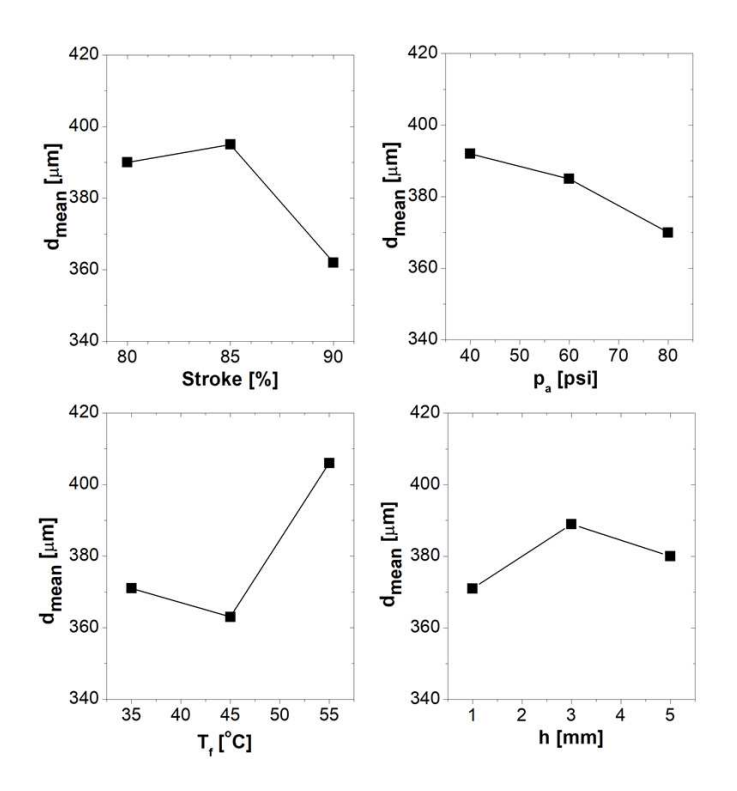


FIGURE 6: PARAMETERS EFFECTS PLOT FOR DROPLET DIAMETER MEANS FROM INITIAL TAGUCHI DOE.

From the data collected in the initial Taguchi DOE, the parameters main effects for signal-to-noise S/N ratios were calculated using eq. (1) (Table 3) and plotted to illustrate the parameter's S/N ration trends with respect to droplet size (Figure 7).

The slope trends in Figure 7 are similar to the ones from Figure 6 but reciprocal or symmetrical with respect to the x-axis". The symmetry of the S/N slopes indicates that there is no significant noise or external factors affecting deposition process Figure 7. Good signal-to-noise ratio indicates good quality in the collected data and rectifies the previous behaviors from Figure 7 and Table 2.

The response for signal-to-noise ratios and ranking for significant effects on the size of adhesive droplet diameter is shown on Table 3.

Table 3: Response Table for Signal to Noise Ratios S/N.

Level	Stroke	Air Pressure [psi]	Temp., T _f	Deposition height, h [mm]
1	-51.83	-51.87	-51.39	-51.32
2	-51.92	-51.68	-51.18	-51.80
3	-51.13	-51.34	-52.17	-51.59
$\Delta S/N$	0.79	0.53	0.99	0.48
Rank	2	4	1	3

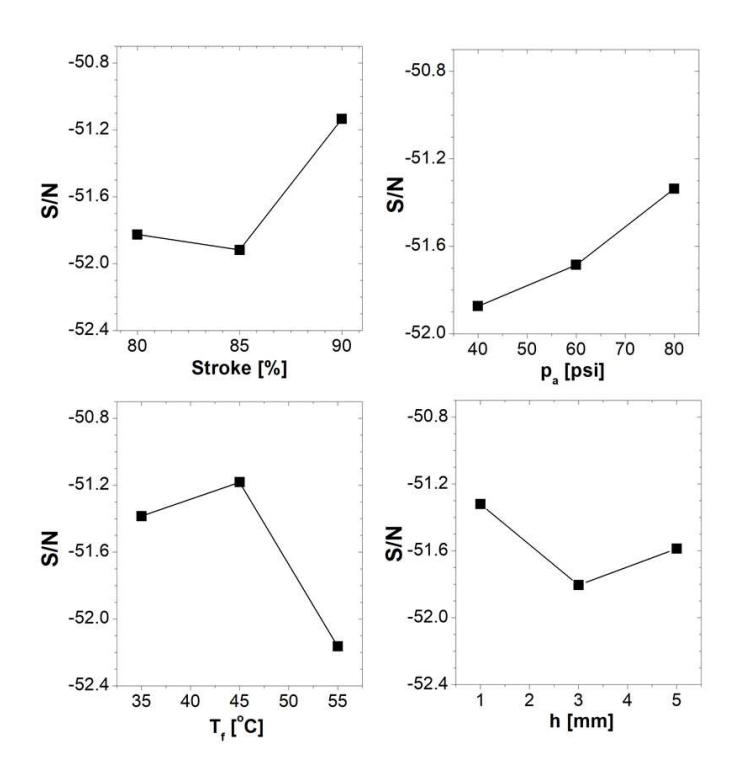


FIGURE 7: PARAMETERS MAIN EFFECTS PLOT FOR SIGNAL-TO-NOISE RATIOS (SN) FROM INITIAL TAGUCHI DOE.

The values displayed in Table 3 for the $\Delta S/N$ indicates how the results for each parameter control affect droplet sizes. Table 3 displays the same level of ranking as in Table 2, Temperature and Instrument's Stroke have the most impact on droplet size, meanwhile Deposition Height and Air Pressure have the least impact on droplet size. After the initial analysis of the Taguchi DOE trials, exploration of trends towards droplet diameter reductions was performed by performing more trial sets. A new trial set consisted of allowing only one parameter to vary in value per trial while the other parameters remained constant for the whole trial set.

Based on the Taguchi DOE data, the deposition height was ranked to have the least impact on the droplet size Nevertheless once we have identified a height value resulting in smaller values of droplet diameter, it could remain constant. This process allows for simplification of new DOEs. The recorded data for three different heights with the other parameters as constants is shown in Table 4 and illustrated in Figure 9.

The largest droplet diameters corresponded to height of 5 mm, meanwhile the lowest corresponded to 1 mm in height. Droplet diameter standard deviation S_d is equal 12.7 μm at 1 mm height, meanwhile droplet diameter S_d is 16.8 μm at 5 mm. It was also noticed on the microscope that at 1 mm height, the droplets are more circular with less splatter in comparison to the samples from 5 mm height. Therefore, decrease in deposition height is resulting not only in adhesive droplets diameter reduction but also better deposition quality.

Table 4: UV adhesive droplet mean diameters with three different heights for trend study. Where: $\overline{d_d}$ – average diameter of deposit (droplet) for the 6 trials, S_d – standard deviation.

Stroke	p _A [psi]	T _f [°C]	h [mm]	$\overline{d_d}$ (μ m)	S _d (µm)
90%	50	35	1	291	12.7
90%	50	35	3	296	11.7
90%	50	35	5	300	10.8

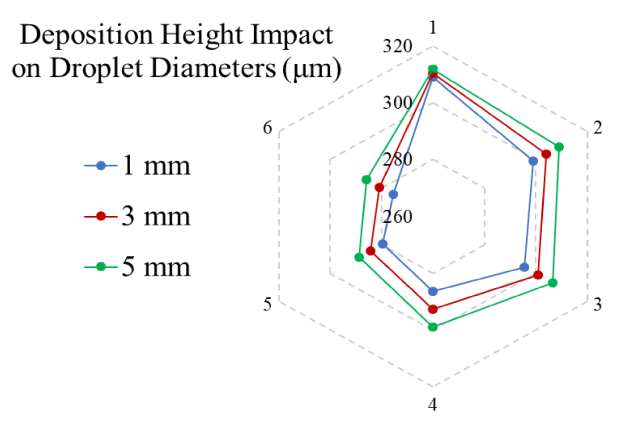


FIGURE 8: CONTOUR PLOT FOR DIFFERENT DEPOSITION HEIGTHS TOWARD DROPLET DIAMETER.

From the Taguchi DOE data, temperature was ranked to have the most impact on the droplet size. Temperature affects the viscosity and density of the adhesive, which influences the flow inside the channel of valve assembly. On other hand change of the viscosity and density due to T_f might influence fluid behavior when forced by cartridge's piston through the nozzle opening.

Table 5: UV adhesive droplet diameters with three different temperatures for trend study.

Stroke	pa [psi]	T _f [°C]	h [mm]	$\overline{d_d}$ (μ m)	S _d (µm)
80%	60	55	1	375	11.2
80%	60	45	3	342	11.3
80%	60	35	5	293	21.9

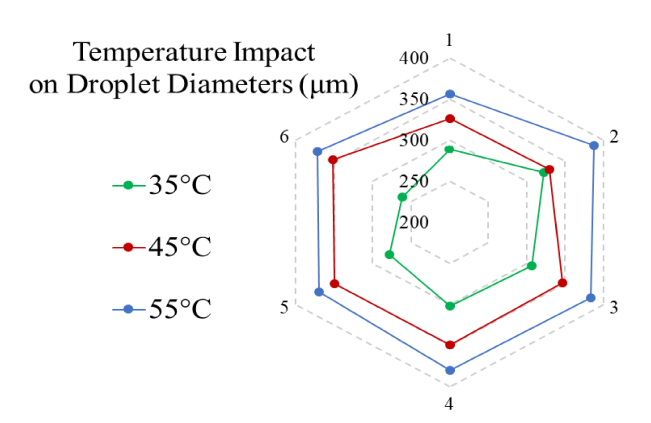


FIGURE 9: CONTOUR PLOT FOR DIFFERENT TEMPERATURES TOWARD DROPLET DIAMETER.

Since too high temperatures (>65 °C) could damage the adhesive syringe, meanwhile low temperatures could cause clogs inside the valve assembly. For practical reasons an operating range for temperature was setup to be between 30°C to 65°C. The recorded data for three different temperatures with the other parameters as constants is shown in Table 5 and illustrated in Figure 9. The highest droplet diameters corresponded to 55°C, meanwhile the lowest corresponded to 35°C with droplet diameters 375 and 293 micron respectively and S_d = 11.2 μm and 21.9 μm respectively. Therefore, decrease in temperature is associated with adhesive droplets diameter reduction.

Table 6: UV adhesive droplet diameters for four different values of stroke for trend study.

Stroke	pa [psi]	T _f [°C]	h [mm]	$\overline{d_d}$ (μ m)	S _d (µm)
85%	60	55	1 mm	416	7.4
80%	60	55	1 mm	375	11.2
70%	60	55	1 mm	366	10.6
65%	60	55	1 mm	286	6.0

The recorded data for four different values of instrument's strokes with the other parameters as constants is shown in Table 6 and illustrated in Figure 10. The highest droplet diameters corresponded to 85% (100V), meanwhile the lowest corresponded to 65% with droplet mean diameters decreasing from 416 to 286 μ m. Therefore, decrease in instrument's stroke is associated with adhesive droplets diameter reduction.

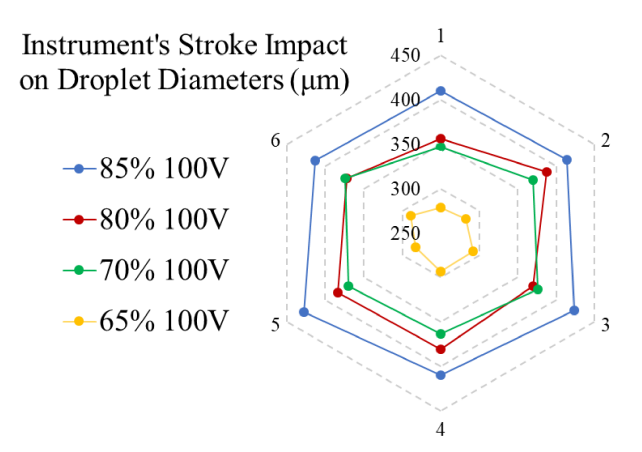


FIGURE 10: CONTOUR PLOT FOR DIFFERENT INSTRUMENT'S PISTON STROKES.

Table 7: UV adhesive droplet diameters with three different air pressures for trend study.

Stroke	pa [psi]	T _f [°C]	h [mm]	$\overline{d_d}$ (μ m)	S _d (µm)
80%	50	35	1 mm	230	30.9
80%	60	35	1 mm	288	31.8
80%	70	35	1 mm	336	61.3

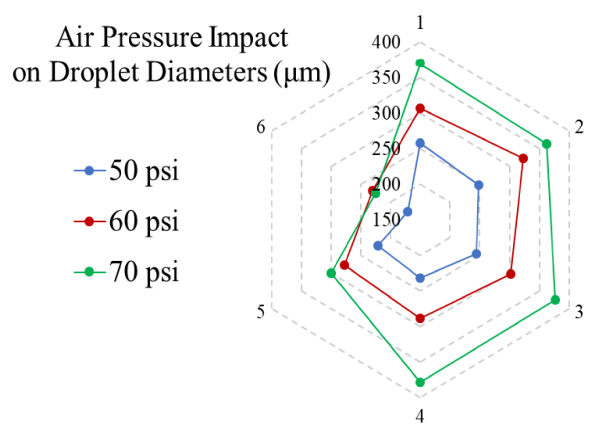


FIGURE 11: CONTOUR PLOT FOR DIFFERENT VALUES OF AIR PRESSURE.

The recorded data for three different air pressures with the other parameters as constants is shown in Table 7 and illustrated in Figure 12. The largest values of droplet diameter corresponded to 70 psi, meanwhile the lowest corresponded to 50 psi with droplet diameters varying from 336 μm to 230 μm . Therefore, decrease of applied air pressure is associated with adhesive droplets diameter reduction.

Table 8: Final optimized results UV adhesive droplet diameters on a glass and Si substrates.

Substrate	Stroke	p _A [psi]	T _f [°C]	h [mm]	$\overline{d_d}$ (μ m)	S _d (µm)
Glass	83%	25	40	1 mm	264	7.4
Si	83%	25	40	1 mm	153	5.2

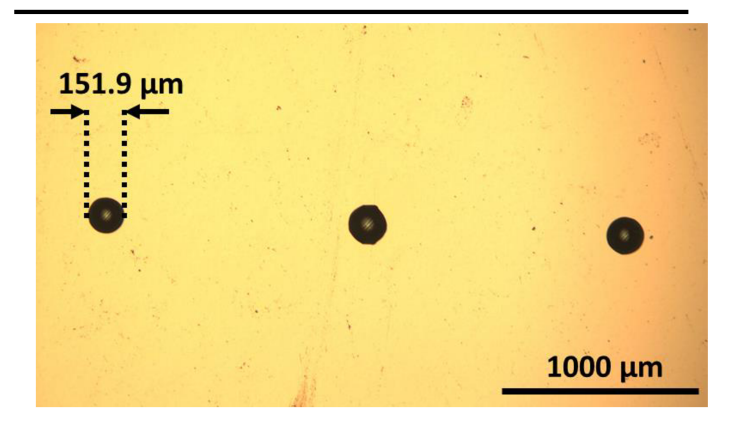


FIGURE 12: UV ADHESIVE DROPLETS ON SILICON (SI) SUBSTRATE WITH DIMETER AROUND 150 MICRON.

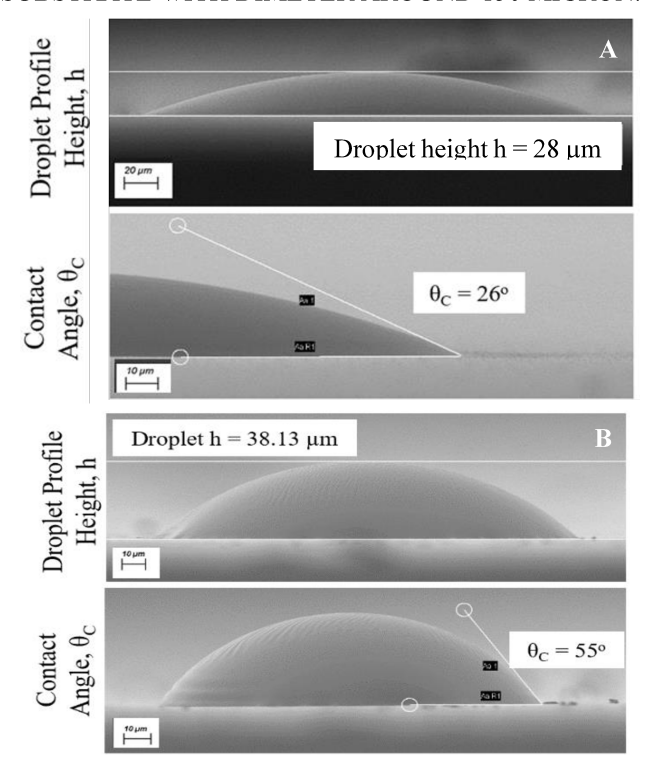


FIGURE 13: UV ADHESIVE DROPLET HEIGHTS AND CONTACT ANGLES ON A) GLASS AND B) SILICON SUBSTRATES.

Based on the last sets of DOE data, we were able to identify parameters trends towards droplet diameter reduction. These trends and parameter values helped to determine a final set of optimized combination of parameters with respect to repeatability and reliability on glass (SiO2) slides. The same set of parameters was tested on a clean (degreased) silicon (Si) substrates which are for of the actual snap-fasteners and our microrobot's components. The recorded data for the last set of trials are shown in Table 8 and deposited droplets shown in Figure 12.

We have determined mean droplet diameter to be 264 μm , on the glass (SiO2) substrate. On the silicon (Si) substrate, the mean droplet diameter was 153 μm . Both trials used the same combination of parameters for deposition on different surfaces (Table 8) (same volume of adhesive released), but droplet diameters on the silicon substrates were usually for about 100 μm smaller than in case of the glass slides. SEM characterization of the of the adhesive deposits on the glass and Si substrates allowed to observe actual shape of the deposits and determine profile height and contact angle between the UV glue and substrate's surface. SEM characterization revealed that for the same volume of released fluid contact angle and profile height of the droplets on Si substrate are significantly larger than in case of the glass substrate (Figure 13) which is consistent with previously observed values of deposit's diameter $d_{\rm d}$.

4. DISCUSSION

4.1 Analysis of the parameters impact on the UV adhesive size.

One of the disadvantages of the Taguchi method is that it does not account for interactions and dependencies between the parameters. Nevertheless, the knowledge about such correlation between parameters might be useful in the optimization of the process. After we have determined that stroke and temperature are the parameters with the strongest impact on the droplet size, the optimal conditions needed to reduce the size of the deposited droplet (Table 8) were determined not only with the help of Taguchi method analysis but also considering possible relation interaction between Stroke and $T_{\rm f}$ in Pico Pulse deposition process.

The value of stroke = 83% (Table 8) is close to the maximum setting of the given parameter for inkjet printer associated with larger droplet diameter. Temperature of 40°C is close to the selected practical minimum temperature of 35°C. Based on the results from testing solely temperature effect on the droplet size we have determined that minimum droplet size is for the 35°C (Table 5). When T_f is increasing diameter of the droplet is increasing as well. This is most likely due to the decrease of the density and viscosity with the increase of the temperature of the fluid. Droplet with reduced density and viscosity would interact differently with substrates surface because of the changes in the surface forces resulting in larger droplet size.

On the other hand, stroke shows different trend, where with decrease of its value droplet size is decreasing as well. This effect can explained based on the deposition mechanism of Pico Pulse. Stroke value affects impact force of the piston on the fluid being pushed through the nozzle. For lower values of the stroke piston's impact force is smaller, for the higher values of the stroke impact force is larger. Considering that impact force of the fluid is directly proportional to the initial velocity of the droplet when released through the nozzle, and in consequence to the momentum and kinetic energy of the free falling droplet – which has to be compensated upon hitting the substrate.

As a result, in ideal situations we would keep temperature of the fluid as low as possible and at the same time use low values of the stroke. However, lower temperatures of the fluid results in higher viscosity and density which need larger force in order to push adhesive through the nozzle. Consequently optimal parameters from Table 8 include values of the three parameters: temperature, deposition height, and pressure closer to the values corresponding to the reduced droplet size as determined from individual tests, and stroke's values related to larger droplet size (Table 6, Figure 10). As noted before, this observations reflects the limitations of the Taguchi method.

4.2 UV adhesive deposition on glass and Si substrates – SEM characterization

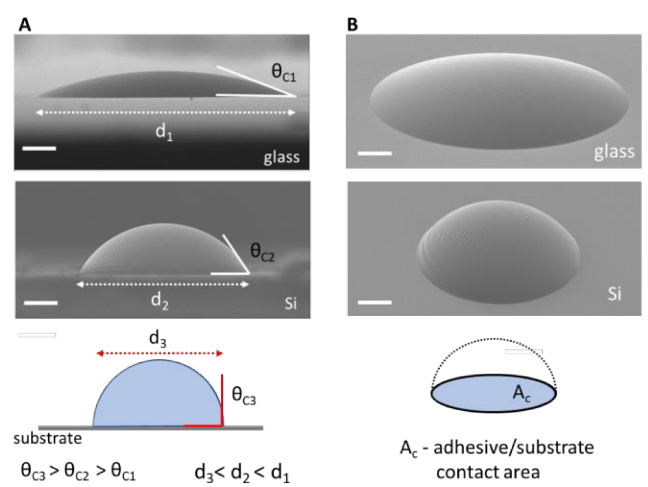


FIGURE 14: WETABILITY EFFECT - RELATION BETWEEN CONTACT ANGLE Θ_C AND DIAMETER (D) OF THE CONTATCT AREA BETWEEN ADHESIVE AND SUBSTRATE. FOUR TOP SEM IMAGES OF THE UV ADHESIVE ON THE GLASS AND SI SUBSTRATES AND ILUSTRATION OF HYPOTHETICAL FURTHER REDUCTION OF THE DIAMETER ON BOTTOM DIAGRAMS. A – PROFILE VIEW, B – TILT VIEW AT 30° . SCALEBAR CORESPONDS TO 30 MICRON.

Scanning Electron Microscope (SEM) characterization and study of the adhesive deposit profiles revealed that droplets on silicon substrates have larger profile heights and contact angles than droplets on glass (Figure 13). This is consistent with the fact that contact area $A_{\rm c}$ of an adhesive and substrate has a smaller diameter on a silicon wafer compared to a glass slides (Figure 14). Observed differences in the size and shape of the deposited adhesive features on a different substrates is due to wettability

effect. Specifically, we have to consider the surface forces between UV adhesive and respective substrate which would result in different values of contact angle at adhesive-substrate interface, profile height, and consequently droplet diameter d_d of a droplet-substrate contact area A_c .

We can speculate that wettability effect can be hypothetically utilized for further reduction of the adhesive-substrate contact area, if we consider other substrate materials and/or various formulation of the adhesive. Depending on the relation between surface forces and adhesion of the given glue material to the substrate, it might be possible to practically realize scenario with larger contact angles, which would correspond to smaller contact area A_c (Figure 14 A, B bottom diagrams). This might enable to use Pico Pulse and other Inkjet printing tools for assembly of the structures with even more reduced footprint [2].

5. CONCLUSION

In this paper we have demonstrated novel applications of the Inkjet printing as the method for controlled dispensing of small volumes of UV adhesive which enables its use in future automated micro assembly tasks. Dispensing of adhesive was realized using a Nordson EFD® Pico Pulse system, which is controlled by a number of process variables. We applied the Taguchi Design of Experiment (DOE) method in order to identify values of the process parameters needed for reducing the size of adhesive droplets (deposits) and conducted characterization of the printed features with the help of optical microscopy and scanning electron microscopy (SEM). Experimental characterization data reveals that UV adhesive droplet deposited on the Silicon substrate has minimum diameter around 150 μm .

We have determined that the instrument's stroke and temperature are the parameters which have the strongest correlation with the changes of deposit diameter as well as quality of the deposits. Future studies of the wettability of the adhesives on different types of the substrates can lead to further reduction of the adhesive droplet size which might expand Inkjet printing application in the assembly of the microstructures.

ACKNOWLEDGEMENTS

The authors would like to thank staff of the MicroNano Technology Center at University of Louisville for providing access to the Scanning Electron Microscope (Zeiss Supra 35). Also we would like to thank Dr Kevin Walsh for providing access to the Olympus BX51 optical microscope at MEMS Research lab at University of Louisville.

REFERENCES

- [1] Popa, Dan O., and Stephanou, Harry E., "Micro and mesoscale robotic assembly." Journal of manufacturing processes, 6, 1, 52-71, (2004).
- [2] Lambert, Pierre, "Capillary Forces in Microassembly: Modeling, Simulation, Experiments, and Case Study", Springer, (2011).

- [3] Jandric, Zoran, et al. "Characterization of assembled MEMS." Reliability, Packaging, Testing, and Characterization of MEMS/MOEMS IV. Vol. 5716. International Society for Optics and Photonics, (2005).
- [4] Das, Aditya N., et al. "Precision alignment and assembly of a Fourier transform microspectrometer." Journal of Micro-Nano Mechatronics 5.1-2, 15, (2009).
- [5] Mayyas, Mohammad, et al. "An Active Micro Joining Mechanism for 3D Assembly" Journal of Micromechanics and Microengineering, vol.19, no.3, (2009).
- [6] Campbell, F.C. "Adhesive Bonding and Integrally Cocured Structure: A Way to Reduce Assembly Costs through Parts Integration." Manufacturing Processes for Advanced Composites, pp. 241–301, (2004).
- [7] Groover, Mikell, P. Fundamentals of Modern Manufacturing: Materials, Processes, and Systems. J. Wiley & Sons, (2010).
- [8] Murthy, Rakesh., Stephanou, Harry E and Popa, Dan O., "AFAM: An Articulated Four Axes Microrobot for Nanoscale Applications," in IEEE Transactions on Automation Science and Engineering, vol. 10, no. 2, pp. 276-284, (2013).
- [9] Zhang, Ruoshi, et al. "Design and characterization of solid articulated four axes microrobot for microfactory applications." Journal of Micro-Bio Robotics 15.2, 119-131, (2019).
- [10] Murthy, Rakesh, Aditya Das, and Dan O. Popa. "ARRIpede: A stick-slip micro crawler/conveyor robot constructed via 2 ½D MEMS assembly." 2008 IEEE/RSJ International Conference on Intelligent Robots and Systems. IEEE, (2008).
- [11] Murthy, R., Das, A. N., Popa, D. O., & Stephanou, H. E. "ARRIpede: An Assembled Die-Scale Microcrawler. Advanced Robotics", 25(8), 965–990, (2011).
- [12] Das, A. N., Murthy, R., Popa, D. O., and Stephanou, H. E.,"A Multiscale Assembly and Packaging System for Manufacturing of Complex Micro-Nano Devices," in IEEE Transactions on Automation Science and Engineering, vol. 9, no. 1, pp. 160-170, (2012).
- [13] Zhang, Ping, Mayyas, Mohammad, Lee, Woo Ho, Popa, Dan O., Shiakolas, Panos, Stephanou, Harry E., Chiao, J. "An active locking mechanism for assembling 3D microstructures", Proceedings of SPIE The International Society for Optical Engineering. 6414. 641425, (2006).
- [14] Lau, Gih-Keong and Shrestha, Milan, "Ink-Jet Printing of Micro-Electro-Mechanical Systems (MEMS)", Micromachines, 8, 194, 2017. [1] Nearing, Anne G. ASME Style Guide, (2018)
- [15] Fribourg-Blanc, Eric, Dang, Dung My Thi, Dang, Chien Mau, "Characterization of silver nanoparticle-based inkjet printed lines", Microsyst Technol 19:1961–1971, (2013).
- [16] Soltman, Dan and Subramanian, Vivek, "Inkjet-Printed Line Morphologies and Temperature Control of the Coffee Ring Effect", Langmuir, 24, 2224-2231, (2008).
- [17] Roy, R. K., A, "Primer on the Taguchi Method", Van Nostrand Reinhold, New York (1990).
- [18] Shih, Hsueh, Ramachandran, Chen, Kumar, Vasant, Glowacki, Bartlomiej A., "Study on chemical-solution-deposited lanthanum zirconium oxide film based on the Taguchi method", J Sol-Gel Sci Technol, 51:102–111, (2009).